

# Improved Motion Stereo Matching Based on a Modified Dynamic Programming

Mikhail Mozerov<sup>1</sup>, Vitaly Kober<sup>1</sup>, and Tae S. Choi<sup>2</sup>

<sup>1</sup>Laboratory of Digital Optics, Institute of Information Transmission Problems, 19 Bolshoi Karetnii, 101447 Moscow, Russia . [mozer@iitp.ru](mailto:mozer@iitp.ru)

<sup>2</sup>Department of Mechatronics, Kwangju Institute of Science and Technology, 572 Ssang-Am Domg, Kwang-San Ku, Kwang-Ju, 506-712, Korea

## Abstract

*A new method for computing precise depth map estimates of 3D shape of a moving object is proposed. 3D shape recovery in motion stereo is formulated as a matching optimization problem of multiple stereo images. The proposed method is a heuristic modification of dynamic programming applied to two-dimensional optimization problem. 3D shape recovery using real motion stereo images demonstrates a good performance of the algorithm in terms of reconstruction accuracy.*

## 1. Introduction

In typical industrial applications, objects are often presented to inspection on a conveyor belt. If multiple snapshots of moving objects are taken by a fixed camera, then the belt motion provides the stereo disparity. This method is referred to as motion stereo [1]. Other methods in which the camera system moves along its optical axis is called axial motion stereo [2]. These methods are useful in applications like autonomous vehicles and manipulation. The correspondence problem is a key point in any stereo vision, or motion analysis task. It is well known that the correspondence problem is inherently ambiguous and some additional information must be added to solve it. Various approaches have been suggested for solving the correspondence problem [3-6]. If the views of two stereo pair images have large differences in visual appearance, then feature-based methods are more suited to image matching [7,8]. On the other hand, area-based methods, for example correlation-based methods, can be alternative to feature-based ones when stereo pair images have a high degree of photometric similarity. For the case of motion stereo, all adjacent image pairs can be matched by using correlation-based methods [9-11]. In general, correlation-based methods are more robust to noise, and they are more suited to efficient implementation on available hardware. The

correspondence based on correlation-based methods between the same points in different stereo images is often formulated as a local (area-based) optimization problem. The local optimization involves a few pixels around the corresponding points in different images. The computational complexity of the optimization is quite low at the expense of a high probability of mismatching. On the other hand, correspondence between the same points in stereo images can be considered as a global optimization problem. In this case, the optimization is a variational task over all pixels of stereo images. So by optimizing a given loss function, a more reliable matching can be obtained. In the case of one-dimensional data, dynamic programming [12] applied along the epipolar line of optical setup can be used for solving optimization problem [13,14]. Recently, a method based on dynamic programming for stereo pair images was proposed [15]. In this paper we deal with stereo motion and extend dynamic programming optimization approach to two-dimensional case. However, since the computational complexity of direct optimization is very high (exponential), a heuristic algorithm with a fast computer implementation is suggested. With the help of motion stereo experiment, we demonstrate a good performance of the algorithm in terms of reconstruction accuracy.

In Section 2 we introduce a new motion stereo algorithm based on a modified dynamic programming. Experimental results with real stereo images are presented and discussed in Section 3. Section 4 summarizes our conclusions.

## 2. Motion stereo algorithm

In this section we describe a new algorithm based on a modified dynamic programming. First, let us consider a scheme of 3D shape recovery system shown in Fig. 1 for motion stereo of a moving object on a conveyor belt. Let us assume that a 3D object moves inside a volume denoted as  $(W_1, W_2, \dots, W_8)$ . The object is taken by a fixed camera as snapshots at discrete positions of the conveyor

belt. Here  $S_1, \dots, S_N, \dots, S_E$  denote the first, intermediate, and last positions of a moving object inside the volume, respectively. Let  $L$  denote the distance between the conveyor belt and camera lens, and  $F$  denote its focal length. Let  $(a, b, c, d)$  be a projection plane. This means that the 3D volume is projected by a camera onto 2D projection images, while the object moves along the  $X$  axis with a fixed displacement. In this way we can obtain  $N$  projection images.

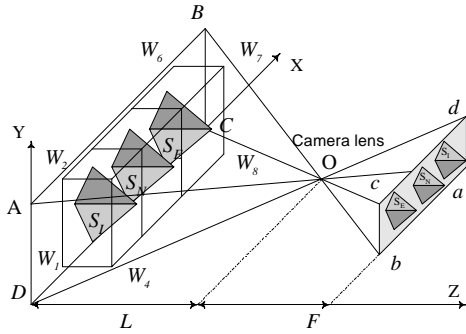


**Fig. 1. Scheme of optical system for motion stereo**

These images are used to reconstruct the surface of a 3D object. Since the reconstruction will be performed by a computer, it is useful to consider a discrete model of motion stereo. When the  $n$ th snapshot ( $n=1, \dots, N$ ) is taken by a camera, the volume can be described by 3D array of  $\{T_{i,j,k}^n; i=0, \dots, I-1, j=0, \dots, J-1, k=0, \dots, K-1\}$ . So  $\{T_{i,j,k}^n; n=1, \dots, N\}$  is time-sequentially projected onto a set of 2D images of  $\{V_{x,y}^n; n=1, \dots, N\}$ . From Fig. 1, it is obvious that the coordinates  $(x,y)$  of  $V_{x,y}^n$  2D image pixel for fixed indices  $(i, j, k)$  can be expressed as follows:

$$\begin{aligned} x_{i,j,k}^n &= \frac{\Delta_I(i - I/2)F + \Delta_X(n-1)}{L - k\Delta_K}, \\ y_{i,j,k}^n &= \frac{\Delta_J(j - J/2)F}{L - k\Delta_K}. \end{aligned} \quad (1)$$

where  $D_K$ ,  $D_I$ , and  $D_J$  are sampling intervals along the  $Z$ ,  $X$  and  $Y$  axes, respectively.  $D_X$  is a shift interval of a moving object along axis  $X$ .

Next the following constraints are taken into account:

- corresponding points lie only on the epipolar line for all images;
- a pixel from one image can correspond only to one pixel in other images;
- light reflection of the 3D object surface is diffuse.

The latter means that an arbitrary small area of the object surface for all positions of the conveyor belt ( $n=1, \dots, N$ ) produces the same reflection intensity values of  $\{V(x_{i,j,k}^n, y_{i,j,k}^n)\}$  on the projection plane. That is

illustrated in Fig. 2. If a point, say  $P$ , belongs to the object surface, then at different conveyor positions this point shown in Fig. 2 as  $P_1, \dots, P_N, \dots, P_E$  produces pixels  $p_1, \dots, p_N, \dots, p_E$  on the projection plane with the same intensity value.

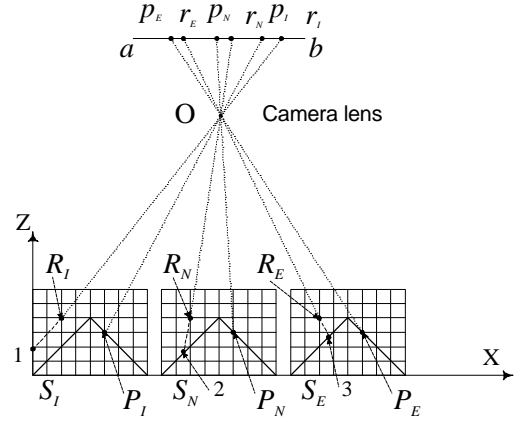


**Fig. 2. Light reflection from the 3D surface of a moving object projected onto a plane**

Conversely, if a point, say  $R$ , shown in Fig. 2 as  $R_1, \dots, R_N, \dots, R_E$  does not lie on the object surface, then the intensity value of corresponding pixels  $r_1, \dots, r_N, \dots, r_E$  on the projection plane can be different. In other words, non-identical surface points, for example 1, 2, 3 in Fig. 2, may have a different light reflection.

We now introduce a dissimilarity function for a set of projection images in the following way:

$$Q_{i,j,k} = \sum_{n=1}^N \sum_{m=n+1}^N |V(x_{i,j,k}^n, y_{i,j,k}^n) - V(x_{i,j,k}^m, y_{i,j,k}^m)| \quad (2)$$

Here the coordinates  $(x,y)$  are computed using Eq. (1).

Let us suppose that the depth map denoted as  $\{h_{i,j}; i=0, \dots, I-1, j=0, \dots, J-1\}$  of a moving object possesses small signal variations. This means that absolute differences between all adjacent elements of the depth map are assumed to be bounded by values of  $Dh_{i,j}$ :

$$|h_{i,j} - h_{i,j-1}| \leq Dh_{i,j}, \quad (3)$$

where  $0 \leq h_{i,j} \leq K-1, i=0, \dots, I-1, j=0, \dots, J-1$ .

Now we formulate optimization problem as follows: find the depth map  $\{\hat{h}_{i,j}; i=0, \dots, I-1, j=0, \dots, J-1\}$  with bounded differences between all adjacent elements given in Eq. (3) in such a way that the sum of the dissimilarity function in Eq. (2) evaluated over all elements of the depth map must be minimal. In other words, it can be written as

$$\hat{h}_{i,j} = \underset{\{h_{i,j}; i=0, \dots, I-1, j=0, \dots, J-1\}}{ARG \ MIN} \left( \sum_{p=0}^{I-1} \sum_{t=0}^{J-1} Q_{p,t} h_{i,j} \right). \quad (4)$$

To give a better understanding of the method, first let us consider optimization of Eq. (4) in the case of one-dimensional data. The problem can be easily solved by using the method of dynamic programming applied along the epipolar line of optical setup. The method consists of step-by-step control and optimization of Eq. (4) according to the Bellman's principle of optimality [12]. The principle is given by a recurrence relation

$$S_{p,h} = \underset{|t| \leq \Delta h_p}{\text{MIN}} (S_{p-1,h+t} + Q_{p,h}), \quad (5)$$

where  $p = 1, \dots, I-1$ , and initial values  $S_{1,h} = Q_{1,h}$ ,  $h = 0, \dots, K-1$ .

So using the recurrence relation in Eq. (5), the minimal value of the criterion in Eq. (4) can be found at the last step of optimization. Next the algorithm works in reverse order and recovers a sequence of optimal steps and the depth map  $\{\hat{h}_i; i = 0, \dots, I-1\}$ .

For the case of two-dimensional data, a direct optimization of Eq. 4 is impractical because the computational complexity of such optimization is exponential. In Section 3, with the help of computer simulation, we also illustrate that optimization of two-dimensional data in Eq. (4) by applying dynamic programming subsequently along the  $I$  and  $J$  discrete axes produces numerous mismatching and errors in 3D-shape recovery.

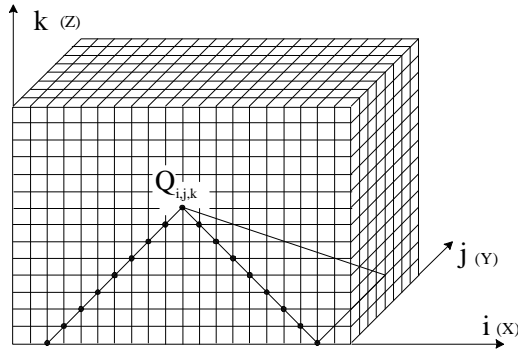


**Fig. 3. Geometrical illustration of three-dimensional dissimilarity function**

Now we consider a new algorithm with a low computational complexity that yields a good performance with respect to 3D shape recovery. The algorithm exploits similar ideas to those of dynamic programming. For a better understanding, a geometrical illustration of the dissimilarity function  $Q_{i,j,k}$  is given in Fig 3. The values of the function geometrically represent a 3D object to be reconstructed in a three-dimensional discrete space ( $I \times J \times K$ ). Here small values of the function correspond to points in the space, which are geometrically close to the object surface. In contrast, large values of the function

correspond to points in the space, which lie far away from the object surface. Next we form a set of matrices from the dissimilarity function by varying index  $j$ ; that is,  $\{W_{i,k}(j) = Q_{i,j,k}; i=0, \dots, I-1, k=0, \dots, K-1, j=0, \dots, J-1, \}$ . If for each matrix of  $\{W_{i,k}(j); j=0, \dots, J-1\}$  a sequence of optimal steps is found by using dynamic programming, then this sequence can be geometrically interpreted as a curve line in the space. As it is mentioned above, a simple accumulation in the space of such lines does not produce a good 3D shape recovery. So we modify dynamic programming method. Let us define a left sum as

$$S_{p,h}^L(j) = \underset{|t| \leq \Delta h_p}{\text{MIN}} (S_{p-1,h+t}^L(j) + W_{p,h}(j)), \quad (6)$$

where  $p = 1, \dots, I-1$ ,  $h = 0, \dots, K-1$ , and initial values  $S_{1,h}^L(j) = W_{1,h}(j)$ ,  $j = 0, \dots, J-1$ .

In a similar manner, a right sum is defined as follows:

$$S_{p,h}^R(j) = \underset{|t| \leq \Delta h_p}{\text{MIN}} (S_{p+1,h+t}^R(j) + W_{p,h}(j)), \quad (7)$$

where  $p = I-2, I-3, \dots, 0$ ,  $h = 0, \dots, K-1$ , and initial values  $S_{I,h}^R(j) = W_{I,h}(j)$ ,  $j = 0, \dots, J-1$ .

Note that by using Eq. (6) we can obtain at each point, say  $(p, j, h)$ , the optimal path including this point with the left minimal sum calculated from 0 to  $p$  along the  $I$  axis, while the  $j$  index is fixed. In a similar manner, Eq. (7) provides the optimal path including this point with the right minimal sum calculated from  $I-1$  to  $p$  along the same axis, while the  $j$  index is fixed. That follows from the Bellman's principle of optimality.

Then a modified recurrence relation is given by

$$S_{p,h}^J(j) = S_{p,h}^L(j) + S_{p,h}^R(j) - W_{p,h}(j), \quad (8)$$

where  $p = 1, \dots, I-1$ ,  $h = 0, \dots, K-1$ ,  $j = 1, \dots, J-1$ .

We obtain a set of matrices of  $\{S_{p,h}^J(j); j=0, \dots, J-1\}$ .

Note that the  $S_{p,h}^J(j)$  value consists of the left minimal sum calculated from 0 to  $p$  and the right minimal sum calculated from  $I-1$  to  $p$ . In other words, using Eqs (6, 7, 8) for each point, say  $(p, j, h)$ , of the discrete space we can compute the optimal path including this point with the minimal sum calculated along the  $I$  axis, while the  $j$  index varies. All of these minimal sums are stored as the set of matrices. In contrast, the result of dynamic programming applied along the  $I$  axis is only one optimal path with a minimal sum, while the  $j$  index is fixed. The physical meaning of  $\{S_{p,h}^J(j)\}$  at each point the discrete space is a measure of belonging the point to the 3D object surface after one-dimensional optimizations along the  $I$  axis. So the set of matrices of  $\{S_{p,h}^J(j); j=0, \dots, J-1\}$  can be

considered as a new dissimilarity function for optimization along the  $J$  axis. We form a set of matrices from this dissimilarity function; that is,  $\{B_{j,k}(i) = S_{j,k}^J(i); j=0, \dots, J-1, k=0, \dots, K-1, i=0, \dots, I-1\}$ . In this case, a recurrence relation can be written as

$$S_{p,h}^{I,J}(i) = S_{p,h}^L(i) + S_{p,h}^R(i) - B_{p,h}(i). \quad (9)$$

Here left and right sums are defined in a similar way to those in Eqs. (7, 8),

$$S_{p,h}^L(i) = \underset{|t| \leq \Delta h_p}{\text{MIN}} (S_{p-1,h+t}^L(i) + B_{p,h}(i)), \quad (10)$$

where  $p = 1, \dots, J-1, h = 0, \dots, K-1$ , initial values  $S_{1,h}^L(i) = B_{1,h}(i), i = 0, \dots, I-1$ , and

$$S_{p,h}^R(i) = \underset{|t| \leq \Delta h_p}{\text{MIN}} (S_{p+1,h+t}^R(i) + B_{p,h}(i)), \quad (11)$$

where  $p = J-2, J-3, \dots, 0, h = 0, \dots, K-1$ , initial values  $S_{J-1,h}^R(i) = B_{J-1,h}(i), i = 0, \dots, I-1$ .

By repeating the procedure described above, we obtain a set of matrices  $\{S_{p,h}^{I,J}(i); i=0, \dots, I-1\}$ . Finally, the depth map can be computed as

$$\hat{h}_{i,j} = \underset{k}{\text{ARG MIN}} (S_{j,k}^{I,J}(i)), \quad (12)$$

where  $i=0, \dots, I-1, j=0, \dots, J-1$ .

So the proposed algorithm consists of the following steps:

- calculate values of the dissimilarity function  $\{Q_{i,j,k}; i=0, \dots, I-1, j=0, \dots, J-1, k=0, \dots, K-1\}$  given in Eq. (2);
- perform the modified dynamic programming along the  $J$  discrete axis using Eqs.(6, 7, 8),  $Q_{i,j,k} \Rightarrow S_{i,k}^J(j)$ ;
- perform the modified dynamic programming along the  $I$  discrete axis using Eqs.(9, 10, 11),  $S_{i,k}^J(j) \Rightarrow S_{j,k}^{I,J}(i)$ ;
- compute the depth map of a 3D object  $\{\hat{h}_{i,j}; j = 0, \dots, J-1, i = 0, \dots, I-1\}$  from Eq.(12).

The computational complexity of the algorithm can be evaluated as  $I \times J \times K \times (2Dh^{\max} + 1)$  arithmetical operations, here  $\Delta h^{\max} = \underset{i,j}{\text{MAX}} (\Delta h_{i,j})$ .

### 3. Experimental results and discussion

In this section experimental results are presented to illustrate the performance of the proposed algorithm. In our experiment a pyramid is a moving 3D object. The height of the pyramid is 0.15 m. Seven snapshots of the moving object are taken by a CCD camera. These images

are shown in Fig. 4. The images are 410 x 210 pixels. The distance from the conveyor belt to the camera objective is  $L = 0.86$  m. The sampling interval along the  $Z$  axis is  $D_K = 7 \times 10^{-4}$  m. The focal length of the camera is 0.061 m.

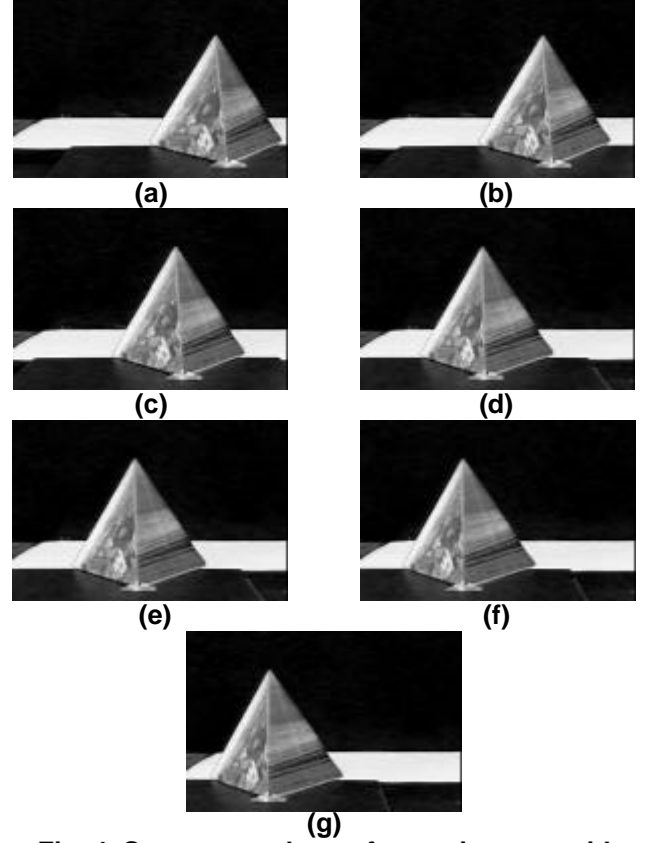


Fig. 4. Seven snapshots of a moving pyramid

In order to obtain a high degree of photometric similarity of motion stereo images, first we equalize their mean and variance values. The depth maps obtained by optimization with the dynamic programming (a) and the proposed algorithm (b) are shown in Fig. 5.

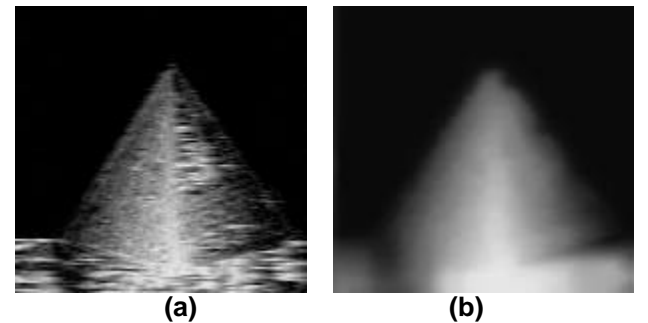
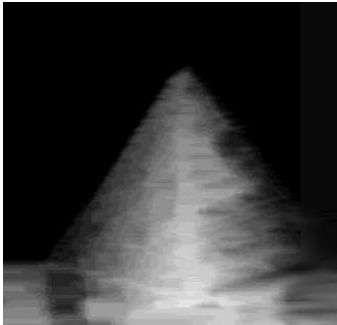


Fig. 5. Depth maps of a moving pyramid obtained on the base of (a) dynamic programming method, (b) modified dynamic programming algorithm

Here gray-scale information of the depth map has the following meaning: the smallest values of the depth map are painted by black color. This means that corresponding elements of the object surface are close to the camera. In contrast, if elements of the object surface are far away from the camera, then values of the depth map are high, and they are painted by white color. We see that 3D shape recovery by the dynamic programming method produces numerous errors, while the proposed algorithm correctly reconstructs the shape of the pyramid.



**Fig. 6. 3D shape recovery of a moving pyramid using modified dynamic programming algorithm with three snapshots**

In order to show how the accuracy of the proposed method depends on the number of motion stereo images, we reconstruct the pyramid using three snapshots of the moving object. The result of reconstruction is presented in Fig. 6. Comparing two results of 3D shape recovery by the proposed algorithm with three and seven snapshots shown in Figs. 6 and 5(b), respectively, we see that the accuracy of reconstruction can be achieved very high by increasing the number of taken snapshots. In general, the accuracy of the suggested method for motion stereo is only restricted by parameters of optical setup.

#### 4. Conclusions

A new motion stereo algorithm based on a modified dynamic programming has been proposed. The reconstruction problem has been formulated as a matching optimization problem of multiple motion stereo images. The accuracy of reconstruction is only restricted by parameters of optical setup, and one can be achieved as high as possible by increasing the number of taken snapshots. Experimental results with real stereo images have demonstrated a good performance of the algorithm in terms of reconstruction accuracy.

Acknowledgment: V. Kober and M. Mozerov acknowledge financial support from the grants 99-01-00265, 99-01-00269 from the Russian Foundation for Basic Research.

#### References

- [1] M. Okutomi and T. Kanade, A multiple-baseline stereo, *IEEE Transactions on Pattern Analysis and Machine Intelligence* **15** (4), 353-363 (1993).
- [2] R.K.K. Yip, A multi-level dynamic programming method for line segment matching in axial motion stereo, *Pattern Recognition*, **31** (11), 1653-1658, (1998).
- [3] D. Marr and T.A. Poggio, A computation theory of human stereo vision, *Proceedings of the Royal Society B* **207**, 301-328 (1979).
- [4] Y. Aloimonos and D. Schulman, Integration of Visual Modules-A Extension of the Marr Paradigm, Academic Press, New York (1989).
- [5] H.K. Nishihara, Practical real-time imaging stereo matcher, *Optical Engineering* **23** (5), 536-545 (1984).
- [6] Y.K.H. Anthony and T.C. Pong, Cooperative fusion of stereo and motion, *Pattern Recognition*, **28** (4), 553-562, (1995).
- [7] G. Medioni and R. Nevatia, Segment-based stereo matching, *Computer Vision, Graphics, and Image Processing* **31**, 2-18, (1985).
- [8] J.H. McIntosh and K.M. Mutch, Matching straight lines, *Computer Vision, Graphics, and Image Processing* **43**, 386-408 (1988).
- [9] H.K. Nishihara and P.A. Crossley, Measuring photolithographic overlay accuracy and critical dimensions by correlating binarized Laplacian of Gaussian convolutions, *IEEE Transactions on Pattern Analysis and Machine Intelligence* **10** (1), 17-30 (1988).
- [10] T. Kanade and M. Okutomi, A stereo matching algorithm with an adaptive window - Theory and experiment, *IEEE Transactions on Pattern Analysis and Machine Intelligence* **16** (9), 920-932 (1994).
- [11] R.J. Woodham, Gradient and curvature from the photometric-stereo method, including local confidence estimation, *JOSA A* **11** (11), 3050-3068 (1994).
- [12] R. Bellman and R. Kalaba, Dynamic programming and modern control theory, Academic, New York (1965).
- [13] S. Lloyd, Stereo matching using intra- and inter-row dynamic programming, *Pattern Recognition Letters* **4** (4), 273-278 (1986).
- [14] Z.N. Lee and J.J. Leou, A dynamic programming approach to line segment matching in stereo vision, *Pattern Recognition*, **27** (8), 961-986, (1994).
- [15] M.G. Mozerov, V.I. Kober, I.A. Ovseyevich, Increasing precision and reducing computational complexity in stereo reconstruction tasks, *Pattern Recognition and Image Analysis* **4**, 116-123, (1994).